Engineered Science
DOI: https://dx.doi.org/10.30919/es1605

Advanced Approaches to Depth Optimization in Large-Diameter Water Well Drilling in Mangystau Peninsula

Gulzada Umirova,[1] Aidar Kuttybayev,[1,*] Volodymyr Khomenko,[2] Samal Muratova,[1] Marian Biletskiy,[1] Boranbay Ratov,[1] Zaida Makhitova,[1] Aigul Gusmanova,[3] Nurbol Tileuberdi,[1,*] Manshuk Sarbopeyeva,[3] Oleksandr Kamyshatskyi[4] and Ligang Zhang[5]

Abstract

Providing a reliable water supply to rural areas of the Mangystau Peninsula requires the construction of large-diameter wells, often in challenging geological conditions. However, the achievable drilling depth is limited by various factors related to hydraulics and the mechanical configuration of the drilling system. This study investigates how key geological and technological parameters influence the maximum depth of large-diameter wells when reverse-circulation drilling is used. A theoretical model was developed to simulate the hydraulic processes within the wellbore and drill string, incorporating variables such as drilling fluid flow rate, rising flow velocity, bit pressure loss, pipe dimensions, and vacuum generated by the pump. The model was used to assess the sensitivity of drilling depth to changes in fluid flow, pipe wall thickness, outside pipe diameter, drilling rate, and vacuum magnitude. The results show that an increase in fluid flow rate or drilling rate significantly reduces the achievable depth due to quadratic growth in hydraulic losses. Conversely, increasing the outer diameter of the drill pipes or the pump vacuum enhances the maximum depth. These findings can help optimize the design of drilling systems for large-diameter water wells and guide future research on cost-effective and deeper well construction in arid regions.

Keywords: Reverse circulation, Water well drilling, Maximum well depth, Increased diameter water well, Mangystau peninsula.

Received: 22 May 2025; Revised: 13 June 2025; Accepted: 18 June 2025.
Article type: Research article.

1. Introduction

Ensuring reliable access to safe drinking water is a critical challenge for rural development in arid regions. The Mangystau Peninsula, with annual precipitation below 150 mm and virtually no surface water, depends almost entirely on groundwater resources.[1,2] However, many aquifers in the region are characterized by complex lithological structures and fractured rock formations that influence water quality and complicate well construction.[3,4] Furthermore, high concentrations of dissolved minerals in several groundwater sources necessitate pre-treatment or desalination before distribution.[5,6]

Accessing fresh groundwater often requires drilling into deep aquifers, which demands specialized techniques capable of penetrating hard rock and maintaining borehole stability.[7–9] Large-diameter well drilling has emerged as an effective solution for increasing intake capacity and lowering operational costs.[10,11] Complementing this approach, reverse circulation systems have been developed to minimize head losses and reduce formation leakage by circulating drilling fluid down the annulus and up through the drill string.[12–15] Such technologies are now widely adopted under complex hydrogeological conditions to enhance drilling efficiency and cuttings removal.[16–18]

Design optimization for water intake wells must account for hydraulic losses associated with partial permeability and structural features of the wellbore.[19–22] In parallel, integrated drilling fluid circulation schemes have been shown to protect sensitive formations and improve cuttings quality in air-lift or pump-assisted modes.[23] Further enhancements in drilling performance have been achieved by optimizing parameters such as weight on bit, rotational speed, and fluid flow rate to

[1] *Satbayev University, 22 Satbaev str., Almaty, 050013, Republic of Kazakhstan*
[2] *Dnipro University of Technology, Ave. Dmytra Yavornytskoho, 19, Dnipro, 49005, Ukraine*
[3] *Yessenov University, microdistrict 32, Aktau, 130000, Republic of Kazakhstan*
[4] *Techpostavka LLC, Kanatnaya st., 130a, Dnipro, 49000, Ukraine*
[5] *Northeast Petroleum University, No. 99, Xuefu Street, High-tech Development Zone, Daqing City, 163318, Republic of China*
**Email:* a.kuttybayev@satbayev.university (A. Kuttybayev); n.tileuberdi@satbayev.university (N. Tileuberdi)

maximize rock-breaking efficiency and extend tool life.[24–26]

Advanced studies of specific mechanisms underpin these improvements. Numerical and experimental investigations of air-lift transport reveal that submergence ratio and annular gap dimensions critically influence liquid-phase velocity and core recovery.[27] Analytical and numerical modeling of asymmetric gas flows beneath drill bits has provided conservative yet practical guidelines for gas injection rates and blade design to optimize bottom-hole cleaning.[28] Research into wear-resistant rock-cutting tools further underscores the need for materials that can withstand abrasive hard-rock conditions.[29–31] Concurrently, fluid flow modeling in reverse circulation devices has demonstrated significant benefits for well-cleaning operations.[32–34]

Insights from polar drilling applications, though in ice rather than rock, offer valuable lessons for managing challenging cuttings removal. Theoretical and experimental models for pneumatic transport of ice core material quantify the air volume and pressure needed for efficient conveyance from deep boreholes.[35] Innovations in dual-wall drill rod systems allow continuous coring with simultaneous cuttings and core removal, enabling rapid penetration in glacier environments.[36] Moreover, mechanisms for autonomous core splitting have been developed to ensure consistent fragment lengths and to evaluate the mechanical effects of ice properties on the breaking process.[37]

Preventive measures learned from neighboring Western Kazakhstan fields emphasize rigorous sealing and well-development protocols to mitigate formation damage.[2] Additionally, using natural-gasoline-based emulsions has enhanced well flow rates and reduced drilling complications in high-mineral-content strata.[38] Optimization of equipment parameters for air-lift and reverse circulation methods significantly lowers energy consumption and operational costs.[18, 39] Detailed analyses of pressure losses during cuttings transport further inform pipe design and fluid selection.[40, 41]

Long-term well productivity also hinges on preventing silt accumulation and degradation of filtration elements. Studies indicate that aging processes reduce the permeability of filter media, prompting the development of novel materials and restoration techniques to extend well life.[42, 43] Attention to the design and deployment of filtration components during drilling is thus crucial for sustained performance.[44, 45]

A multiphase flow model combined with machine learning to evaluate the efficiency of wellbore cleaning by analyzing particle transport mechanisms was presented.[46] The identified dependence of cleaning efficiency on fluid viscosity and flow structure, particularly the role of spiral upward motion, is directly relevant to large-diameter water well drilling, where removal of drilled cuttings is critical for maintaining borehole stability and depth accuracy. The proposed KNN-based model provides a data-driven approach that can enhance decision-making during flushing operations in deep and wide wells.

The microscopic interactions between flushing fluids and solid contaminants using molecular dynamics and machine learning were investigated.[47] The demonstrated improvement in surface wettability and suppression of re-adsorption through surfactant action supports the selection and optimization of effective flushing fluids. These findings are applicable to the design of efficient well-cleaning strategies in water well drilling under complex geological conditions, contributing to improved flushing performance and reduced contamination during depth optimization.

A pressure model for air-lift reverse circulation drilling, emphasizing the role of dual-wall drill pipe depth in optimizing lifting efficiency was developed.[48] These insights are applicable to large-diameter water well drilling, where proper circulation and pressure balance are essential for stable and cost-effective construction at depth.

A machine learning model to predict the performance of drilling fluids in enhancing penetration and preventing fluid losses was introduced.[49] The proposed XGBoost-based approach can support the selection of optimal fluid formulations in water well drilling, especially under variable geological conditions where drilling efficiency and fluid control are critical.

Thus, accounting for geological and technological factors and adopting modern drilling methods and technologies substantially enhance the efficiency of large-diameter wells for water supply in rural areas of the Mangystau Peninsula.[50] Future research in this area should aim to develop integrated solutions that address the region's specific characteristics while leveraging the latest advancements in drilling and water extraction technologies. The development and implementation of such solutions could significantly contribute to the sustainable development of rural areas in the region.

This work aims to analyze the relationships between key drilling parameters, such as drilling depth, drill pipe dimensions, and fluid dynamics, to optimize the design and operational strategies for well drilling with reverse circulation. By investigating the effects of pipe wall thickness, external pipe diameter, and fluid flow characteristics, the study aims to provide theoretical insights that enhance drilling efficiency, reduce pressure losses, and extend the achievable well depth.

2. Materials and methods

This study is based on a theoretical investigation of hydraulic and mechanical factors influencing the maximum drilling depth of large-diameter wells using reverse-circulation drilling techniques. The following subsections describe the methodology and assumptions applied to obtain and analyze the results.

The study employs a system of interrelated mathematical equations to model the reverse-circulation drilling process. The calculations were based on a balance of vacuum pressure and hydraulic losses. Key relationships include:

1. The total vacuum created by the pump, which is distributed between pressure losses in different sections of the circulation system.

2. The dependence of pressure losses on flow velocity, pipe dimensions, and drilling fluid density.
3. The equation for the density of the upward flow, which is affected by cuttings concentration and drilling rate.

The theoretical framework employed for this research is based on the fundamental principles of fluid mechanics and drilling engineering. The relationships between drilling parameters, such as fluid flow rate, drill pipe diameter, wall thickness, and vacuum pressure, were derived using standard equations of hydraulics and pressure loss calculations.

The following assumptions were made to simplify the modeling process and ensure analytical clarity:
1. The drill pipe and casing materials are isotropic, with uniform properties across their length.
2. Pressure losses in the system are evenly distributed across the drill pipe's smooth and jointed sections.
3. The maximum vacuum pressure achievable by the pump is limited by operational wear and environmental conditions.
4. The input parameters for the models were sourced from the technical specifications of drill pipe manufacturers and industry standards. Established equations for pres-sure loss in drilling fluid circulation were utilized, referencing literature providing validation for the theoretical formulations.

The study involved a parametric analysis of five key variables:
Flow rate (Q): Evaluated at values from 1000 to 4000 L/min to assess the impact of increasing circulation intensity.
Drilling rate (ROP): Examined in relation to flow density and its effect on pressure losses.
Vacuum pressure (V): Ranged from 50000 to 85000 Pa to simulate realistic and idealized pump capabilities.
Pipe wall thickness (δ): Analyzed for 168 mm pipes at wall thicknesses from 7 mm to 12 mm.
Outer pipe diameter (dO): Examined using values corresponding to both standard drill pipes and casing pipes used as drill strings in large-diameter wells.

The derived mathematical models were implemented and solved using numerical methods. Calculations were performed for various scenarios, including changes in wall thickness, external diameter, and fluid flow rate. Python and MATLAB software were utilized for computation, with custom scripts written to simulate the effects of varying parameters on maximum drilling depth.

All data supporting the findings of this study are available within the article. As this is a theoretical study, no external datasets or experimental results were produced. The computational formulas and methodologies can be provided upon request to ensure reproducibility and transparency.

3. Results and discussion

3.1 Factors influencing the drilling depth of large-diameter wells using reverse-suction circulation

In reverse-suction circulation, its driving force is the vacuum V generated by the pump. This vacuum is utilized to overcome hydraulic resistances in the suction hose P_{SH}, the Kelly P_K, the drill string P_P, the joints between drill pipes P_J, the drill bit P_B, the annular space between the wellbore walls and the drill string P_{RS}, and the discharge hose P_{DH} (Eq. (1)):

$$V = P_{SH} + P_K + P_P + P_J + P_B + P_{RS} + P_{DH} \quad (1)$$

All components, except P_J and P_B, are determined using the Darcy-Weisbach equation, which for a circular cross-section channel is expressed as (Eq. (2)):[51]

$$P = \rho \lambda L \frac{U^2}{2d} \quad (2)$$

where ρ is the fluid density, λ is the hydraulic resistance coefficient, L is the channel length, U is the flow velocity, and d is the channel diameter.

The hydraulic resistance coefficient is determined using the Reynolds number. During the drilling of large-diameter water wells, circulation is typically performed with water.[52] The Reynolds number can be calculated as follows (Eq. (3)):[53]

$$Re = \frac{\rho U d}{\eta} \quad (3)$$

where η is the dynamic viscosity coefficient.
The flow velocity in the channel is determined as (Eq. (4)):

$$U = \frac{Q}{F} \quad (4)$$

where Q is the fluid flow rate, and F is the cross-sectional area of the channel (Eq. (5)).

$$F = \frac{\pi}{4} d^2 \quad (5)$$

In cases where the Reynolds number exceeds the critical value (for large-diameter water well drilling with drill pipes, $Re_{cr}=10^5$ can be assumed,[54,55] fluid flow occurs in a turbulent regime. Typically, the upward flow velocity in the drill string is maintained at a level that ensures a turbulent regime (Table 1). In this case, the hydraulic resistance coefficient is determined as (Eq. (6)):[56]

$$\lambda = \frac{0.0121}{d^{0.226}} \quad (6)$$

The pressure losses in the drill pipe joints are calculated as (Eq. (7)):

$$P_J = \beta \left[\left(\frac{d_P}{d_J} \right)^2 - 1 \right]^2 \rho \frac{(U_J - U_P)^2}{2} \cdot \frac{H}{L_P} \quad (3)$$

where β is a coefficient accounting for the type of drill pipe joints, with β=2 for tool joint joints;[57] d_P and d_J are the internal diameters of the drill pipes and their joints, respectively; U_P and U_J are the fluid velocities in the drill pipes and their joints; H is the well depth; and L_P is the length of a single drill pipe. The fraction after the multiplication symbol represents the number of joints in the drill string.

In reverse circulation, no nozzles are used on the drill bit, as the fluid flows around the bit externally—therefore, P_B can be neglected. Similarly, P_{RS} can be ignored because, due to the large annular space area, these losses are negligible (Eq. (4)). Considering the above, Eq. (1) can be rewritten as (Eq. (8)):

$$V = P_{SH} + P_K + P_P + P_J + P_{DH} \quad (8)$$

Let us express Eq. (8), first isolating its depth-dependent terms, P_P and P_J, and then those independent of depth (Eq. (9)):

$$V = H\lambda\rho\frac{U_p^2}{2d_p} + 2\left[\left(\frac{d_p}{d_J}\right)^2 - 1\right]^2 \rho\frac{(U_P - U_J)^2 H}{2l_p} + (L_{HS} + L_{HD} + L_K)\lambda\rho\frac{U_p^2}{2d_P} \quad (9)$$

The term following the second plus sign represents the sum of the pressure losses P_K, P_{HS}, and P_{HD}. The sum in parentheses determines the total length L_{KH} of the respective elements (L_{HS}, L_{HD}, L_K are the lengths of the suction hose, discharge hose, and leading drill pipe, respectively). Their diameters must match the diameter of the drill pipe flow channel d_P in accordance with recommendations.[58, 59]

We can simplify Eq. (9) as follows (Eq. (10)):

$$V = \rho\left\{H\left[\lambda\frac{U_p^2}{2d_p} + 2\left[\left(\frac{d_p}{d_J}\right)^2 - 1\right]^2 \frac{(U_P - U_J)^2}{2L_p}\right] + L_{KH}\lambda\frac{U_p^2}{2d_P}\right\} \quad (10)$$

Let us solve Eq. (10) with respect to the well depth H (Eq. (11)):

$$H = \frac{V - L_{KH}\lambda\rho\frac{U_p^2}{2d_P}}{\rho\left\{\lambda\frac{U_P^2}{2d_P} + 2\left[\left(\frac{d_P}{d_J}\right)^2 - 1\right]^2 \frac{(U_P - U_J)^2}{2L_p}\right\}} \quad (11)$$

Eq. (11) represents the dependence of the drilling depth H of large-diameter wells using reverse circulation on the influencing factors specified in the formula.

Table 1: Parameters of a typical water well.

Parameter	Formula	Unit	Value
Roof depth of aquifer, H_F		m	30
Aquifer thickness, m		m	5
Aquifer head, h_S		m	20
Well flow rate, Q_W		m^3/s	0.005
Drawdown, Δ		m	9
Well depth, H_m		m	40
Enclosing rock density, ρ_F		kg/m^3	2600
Well diameter, D		m	1.50
Length of one drill pipe, L_P		m	10
Outer diameter of drill pipes, d_O		m	0.168
Inner diameter of drill pipes, d_P		m	0.150
Area of drill pipe bore, F_P	(5)	m^2	0.0177
Inner diameter of drill pipe joints, D_J		m	0.128
Area of bore of joints, F_J	(5)	m^2	0.0129
Length of kelly, L_K		m	11
Length of suction hose, L_{HS}		m	15
Length of discharge hose, L_{HD}		m	2
Total length of kelly and hoses, L_{KH}		m	28
Drilling fluid flow rate , Q		m^3/s	0.05
Density of drilling fluid, ρ		kg/m^3	1157
Dynamic viscosity coefficient of drilling fluid, γ		N·s	0.0001
Rate of penetration, ROP		m/s	0.00278
Pump suction vacuum, V		Pa	70000
Flow velocity in drill pipes, U_P	(4)	m/s	2.83
Flow velocity in joints, U_J	(4)	m/s	3.89
Reynolds criterion, Re	(3)		5.66·106
Hydraulic resistance coefficient, λ	(6)		0.0186*
Pressure loss in the leading pipe and hoses, P_{KH}	(2)	Pa	16180
Pressure loss in joints, P_J	(7)	Pa	1570
Pressure loss in drill pipes, P_P	(2)	Pa	53910
Maximum drilling depth, H	(11)	m	91

[1] The Reynolds number exceeds the lower boundary of the turbulent regime by more than an order of magnitude, $Re>10^5$. Therefore, the coefficient λ is the same for both the drill pipes and hoses, as the diameter of the channel is assumed to be the same.

The typical values of the influencing factors for the conditions of the peninsula, as presented in Table 1, are used as baseline values in the calculations.[1,4,7,30,60]

Let's determine the dependence of the maximum drilling depth on various factors included in Eq. (11). Specifically, these factors are the pump flow rate Q, the upward flow velocity U_P, the rate of penetration (ROP), the vacuum created by the pump V, the pipe wall thickness δ, and the outer diameter of the drill pipe d_O.

When establishing the dependence on a specific factor A, the value of A is varied both upwards and downwards from its baseline value by a given step ΔA, limited by the maximum and minimum values—A_{MAX} and A_{MIN}. Exceeding these limits would contradict the capabilities of the adopted drilling technology.

The step size for changing the influencing factor A must ensure a smooth dependence. The step size is determined as Eq. (12):

$$\Delta_A = \frac{A_{max} - A_{min}}{n} \quad (12)$$

where n is the number of steps.

The values independent of the considered influencing factor, *i.e.*, those that remain unchanged during any step, are taken from Table 1. Thus, when establishing each specific dependence on parameter A, the following steps are performed:

1. Identify the parameters of external conditions that are independent of the considered influencing factor.
2. Set the minimum and maximum values of the influencing factor A_{MIN} and A_{MAX}.
3. Set the number of steps.
4. Determine the step size ΔA for the influencing factor.

For each step in changing the factor A, perform the calculations using Eq. (11).

3.2 Dependence of the maximum drilling depth H on the pump flow rate Q and the upward flow velocity U_P

The values that remain constant for any steps in changing the fluid flow rate are V, L_{KH}, L_P, L_P, d_P, F_P, d_J, F_J, ρ, γ, λ. The symbols used in Table 2 represent the following quantities: Q is the flow rate of the drilling fluid; U_P is the flow velocity of the fluid in the smooth section of the drill pipe, as well as in the leading drill pipe and hoses; U_J is the flow velocity in the joints; P_{KH}, P_P, P_J are pressure losses in the Kelly and hoses, in the drill pipes, and in their joints, respectively.

From Table 2, it can be seen that when the fluid flow rate is increased from 1000 to 4000 L/min, *i.e.*, 4 times, the maximum drilling depth decreases from 1190 to 49 meters, *i.e.*, 24 times.

The explanation for this fact can be found by analyzing dependence (Eq. (11)). The vacuum created by the pump V is consumed by two components. The first component – the sum P_P and P_J (Eq. (9)) – includes depth H. The second component, P_{KH}, does not depend on the depth. The first component is the remainder (Eq. (11)) after subtracting the second component, the growth of which reduces this remainder from step to step. In turn, the first component, which decreases for the above reason, is the product of depth H and a multiplier whose value increases with the flow rate, which causes a decrease in the second multiplier, *i.e.*, depth H.

Thus, there are two factors causing a decrease in the maximum drilling depth, and the steepness of the decline is explained by the fact that both factors increase proportionally to the square of the flow rate. Fig. 1 shows the dependence of maximum drilling depth H and pressure losses in the smooth section of the drill pipes P_P on the fluid flow rate Q.

As shown in Fig. 1, the required pressure at the pump outlet gradually decreases from 0.066 MPa to 0.044 MPa, which may seem counterintuitive. However, this is explained by the fact that increasing flow rates reduces the achievable drilling depth, which in turn lowers the total hydraulic resistance along the shortened fluid circulation path. Fig. 1 highlights a key trade-off in the design and operation of reverse-circulation drilling systems. While higher flow rates improve cuttings transport efficiency, they drastically limit drilling depth due to excessive pressure losses. These results emphasize the need for careful flow rate optimization to ensure both effective hole cleaning and maximal achievable depth.

Table 2: Dependence of the maximum well depth H on the drilling fluid flow rate.

Step number	Q, L/min (m^3/s)	U_P, m/s (4)*	U_J, m/s (4)	H, m (11)	P_{KH}, Pa (2)	P_J, Pa (7)	P_P, Pa (2)
0	1000 (0.0167)	0.950	1.290	1190	1560	1980	66460
1	1500 (0.0250)	1.420	1.940	515	3500	1940	64560
2	2000 (0.0333)	1.890	2.580	281	6210	1850	61940
3	2500 (0.0417)	2.360	3.230	169	9700	1740	58560
4	3000 (0.0500)	2.830	3.890	106	14010	1620	54340
5	3500 (0.0583)	3.310	4.520	73	19050	1480	49470
6	4000 (0.0667)	3.790	5.171	49	24940	1300	43760

[1] In parentheses, the calculation formulas are provided.

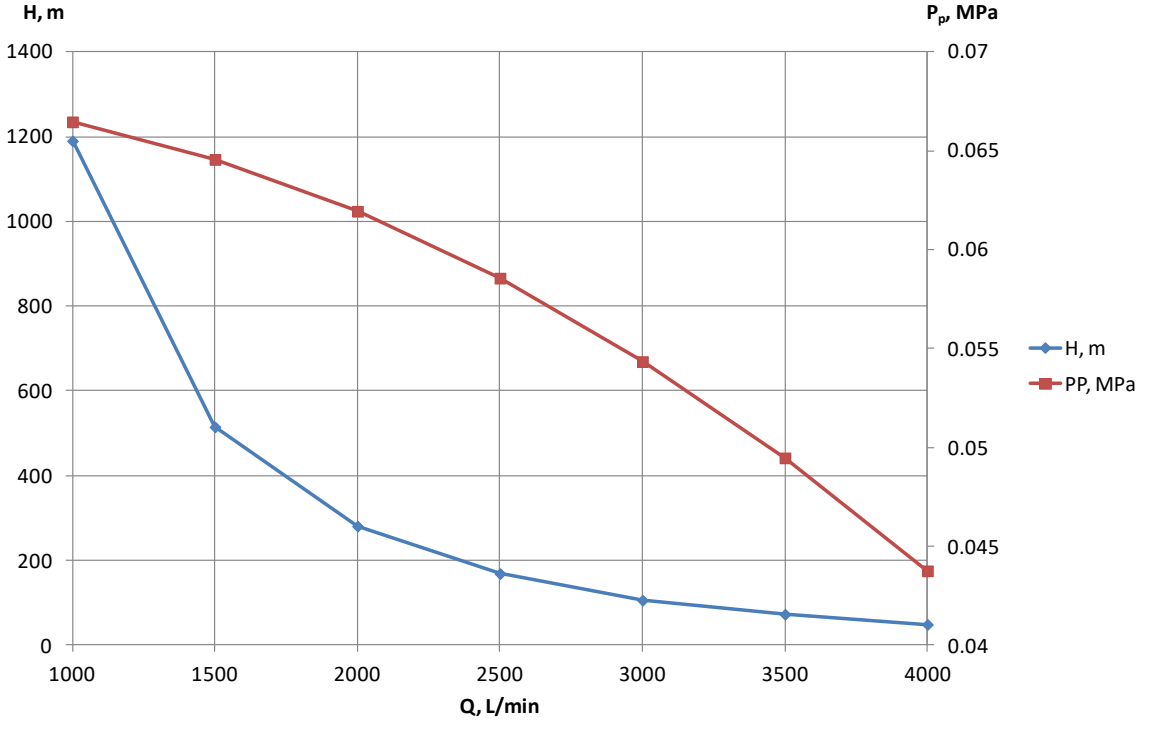

Fig. 1: Dependence of maximum drilling depth H and pressure losses in the smooth section of the drill pipes P_P on the fluid flow rate Q.

3.3 Dependence of the maximum drilling depth H on the drilling rate ROP

This task is solved through the density of the upward flow, establishing its dependence on the drilling rate. The increase in density for reverse circulation (Eq. (13)) is defined based on the formula,[61] developed for direct circulation:

$$\Delta_F = \frac{D^2(\rho_F - \rho_W)ROP}{d_P^2 U_P} \quad (13)$$

where D is the well diameter; d_P is the inner diameter of the drill pipes; ρ_F is the density of the rock; ρ_W is the density of the drilling fluid (water); ROP is the drilling rate; and U_P is the upward flow rate.

Table 3 and Fig. 2 show the dependence of the density of the upward flow ρ and the drilling depth H on the ROP.Using Eq. (13) to derive the dependence of upward flow density ρ on the ROP, and applying Eq. (11), we examine the desired dependence of maximum depth on the drilling rate. The values remaining constant for any changes in drilling rate are: V, D, dP, dJ, λ, UP, UJ, ρF, LKH, LP (Table 1).

Table 3 demonstrates that the decline in maximum drilling depth with an increase in the drilling rate (and the corresponding increase in fluid density) has an inversely proportional nature. Indeed, at each step of the drilling rate increase, the depth decreases by 3 meters.

Table 3: Dependence of the maximum well depth H on the ROP.

Step number	ROP, m/h (m/s)	ΔP, kg/m³	P, kg/m³	H, m (11)	P_{KH}, Pa (2)	P_J, Pa (7)	P_P, Pa (2)
0	2 (0.00056)	32	1032	105	14460	1620	53920
1	4 (0.00111)	63	1063	101	14890	1605	53500
2	6 (0.00167)	95	1094	97	15320	1590	53080
3	8 (0.00222)	125	1125	94	15750	1575	52660
4	10 (0.00278)	157	1157	91	16180	1560	52240
5	12 (0.00333)	187	1187	88	16610	1545	51820
6	14 (0.00389)	219	1219	85	17040	1530	51400
7	16 (0.00444)	250	1250	82	17470	1515	50980
8	18 (0.00500)	281	1280	79	17900	1510	50560
9	20 (0.00556)	313	1310	76	18330	1500	50140

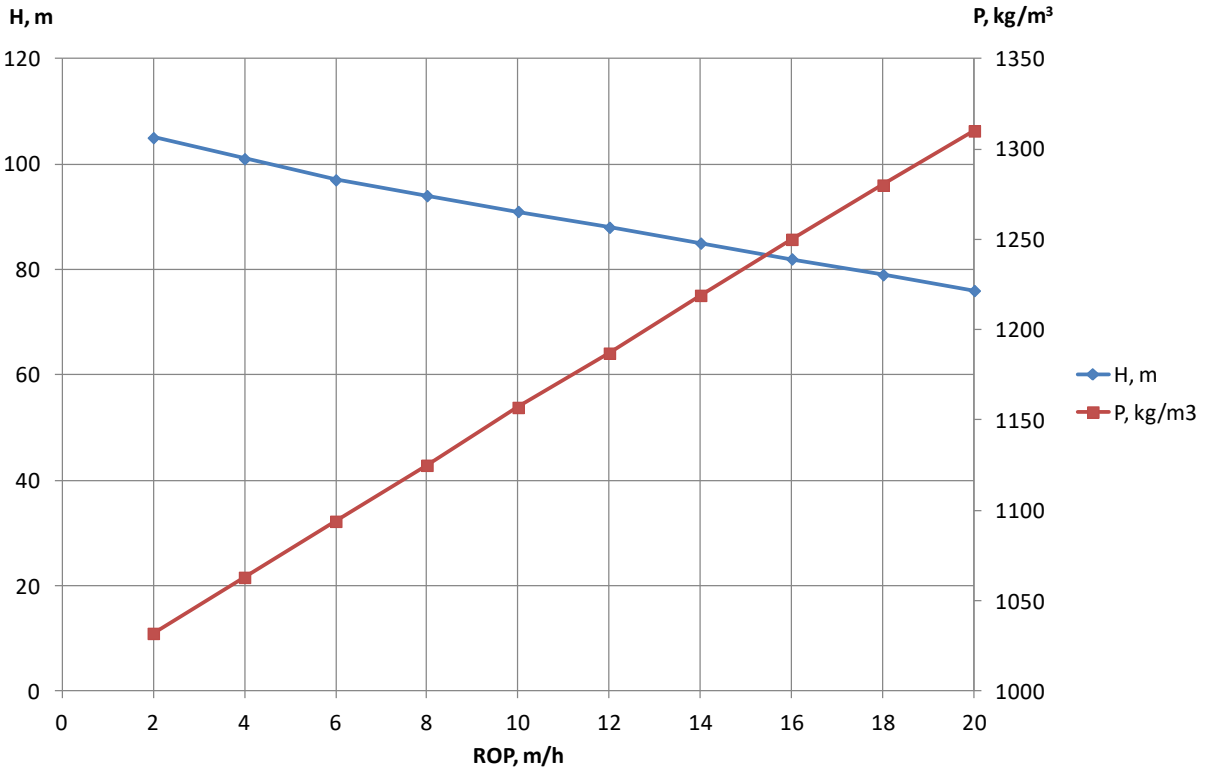

Fig. 2: Dependence of the density of the upward flow ρ and the maximum drilling depth H on the ROP.

The data in Fig. 2 reveal that as ROP increases from 2 to 20 m/h, the maximum drilling depth decreases from approximately 105 m to 76 m. This inverse relationship can be attributed to the greater cuttings generated at higher penetration rates, which require more effective hydraulic transport. To compensate for this, the density of the drilling fluid must be increased from around 1032 kg/m³ to 1310 kg/m³ to maintain adequate carrying capacity and ensure borehole stability.

Therefore, while higher penetration rates can improve productivity, they also impose greater hydraulic demands, limiting achievable depth unless fluid properties are adjusted accordingly. These findings emphasize the importance of integrated control of ROP and fluid characteristics in optimizing drilling performance, especially in large-diameter wells with reverse circulation.

3.4 Dependence of maximum drilling depth H on the vacuum V created by the pump

As is known, achieving an ideal vacuum of one atmosphere is unattainable with standard pump operations. Additionally, during reverse circulation drilling, the working elements of the centrifugal pump are continuously exposed to drilling cuttings, leading to wear on the components. Viscous rock particles adhere to the blades, and impacts from larger particles can deform these components—all of which inevitably reduce the vacuum level originally designed for this type of pump. Table 4 illustrates the dependence of the maximum well depth H on the vacuum V generated by the pump. Fig. 3 depicts the relationship between pressure losses in the drill pipes P and the drilling depth H with respect to the vacuum V created by the pump.

Table 4: Dependence of maximum well depth H on the vacuum V generated by the pump.

Step number	V, Pa	H, м (12)	V - P_{KH}, Pa	P_J, Pa (8)	P_P, Pa (2)
0	50000	57	33820	1000	32820
1	55000	65	38820	1140	37680
2	60000	74	43820	1300	42520
3	65000	82	48820	1440	47360
4	70000	91	53820	1560	52230
5	75000	99	58820	1730	57090
6	80000	107	63820	1870	61950
7	85000	116	68820	2030	66790

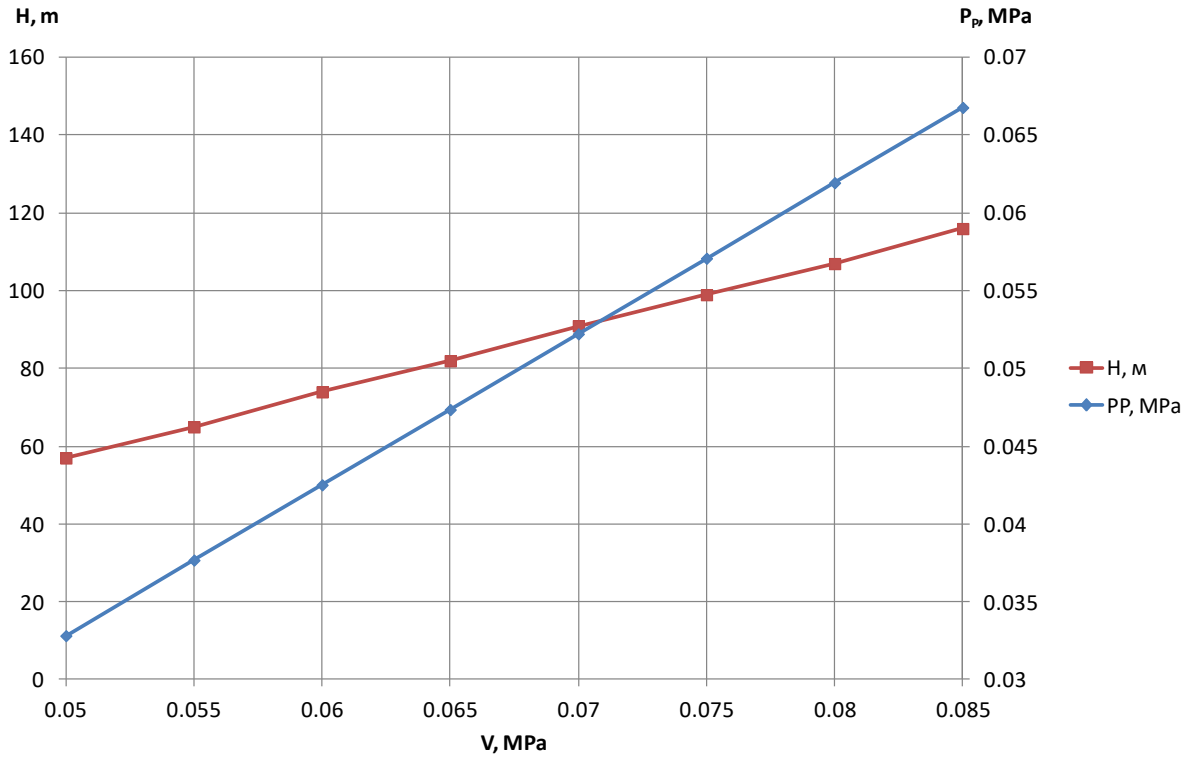

Fig. 3: Dependence of pressure losses in drill pipes P_P and maximum drilling depth H on vacuum V created by the pump.

The values that remain constant with changes in vacuum include d_P, d_J, λ, ρ, Q, U_P, U_J, ROP, L_{KH}, L_P, P_{KH} (Table 1). When subtracting the vacuum-independent value of P_{KH}, equal to 16180 Pa, at each step, all values listed in Table 4 increase in direct proportion to the vacuum.

As shown in Fig. 3, the growth of the maximum drilling depth as the vacuum increases. It steadily increased from approximately 57 m at 0.05 MPa to about 116 m at 0.085 MPa. This indicates that creating a higher vacuum enhances the ability to reach greater depths by improving fluid removal efficiency and reducing the bottom-hole pressure.

Simultaneously, pressure losses in the drill pipes also rise with increasing vacuum, from roughly 0.033 MPa to 0.067 MPa. This increase is due to the higher flow rates and frictional resistance required to maintain effective reverse circulation under greater vacuum levels.

3.5 Dependence of maximum drilling depth H on pipe wall thickness δ

When varying the wall thickness, the following parameters remain constant: d_O, V, d_J, λ, ρ, Q, U_J, L_{KH}, L_P (Table 1). Let us consider this dependence for drill pipes with a diameter of 168 mm. These pipes are manufactured with five wall thickness values:[62,63] 7.5, 8.0, 8.9, 10.6, and 12.1 mm. For simplicity, we examine a model where the thickness varies within this range but in 1 mm increments, *i.e.*, 7, 8, 9, 10, 11, and 12 mm. Table 5 presents the calculated results for the dependence of maximum well depth H on the wall thickness δ of 168 mm drill pipes. Fig. 4 illustrates the relationship between pressure losses in drill pipe joints P_J and the drilling depth H with respect to the wall thickness δ of the drill pipe.

With a maximum reduction in the channel diameter d_P by a factor of 1.07 due to an increase in wall thickness δ, its cross-

Table 5: Dependence of the maximum well depth H on the wall thickness δ of the drill pipe 168 mm.

δ_P, mm	d_P, mm	F_P,* m^2	U_P, m/s (4)	H, m (11)	P_{KH}, Pa (2)	P_P, Pa (2)	P_J, Pa (7)
7	0.154	0.01863	2.6838	100.8	14467	52154	3377
8	0.152	0.01815	2.7548	96.2	15243	52371	2395
9	0.150	0.01767	2.8297	91.0	16083	52270	1638
10	0.148	0.01720	2.9070	85.6	16974	51890	1079
11	0.146	0.01674	2.9869	80.3	17919	51392	682
12	0.144	0.01629	3.0693	75.0	18922	50685	405

* F_P is area of the channel of drill pipes, leading pipe and hoses

sectional area F_P decreases proportionally to the square of this reduction—by a factor of 1.145. This also leads to an increase in flow velocity U_P. Pressure losses P_{KH} rise proportionally to the square of the velocity, *i.e.*, by a factor of 1.30. Pressure losses in the smooth section of the drill pipe decrease by a factor of 1.03, which is relatively small due to the reduction in the corresponding length H by a factor of 1.36.

As shown in Fig. 4, the maximum drilling depth as the wall thickness of the drill pipe increases. At a wall thickness of 7 mm, the maximum drilling depth reaches approximately 101 m. As the wall thickness increases to 12 mm, the maximum depth drops to around 74 m. This trend reflects the impact of increased structural resistance and potential hydraulic limitations associated with thicker-walled pipes, which reduce the efficiency of cuttings removal and circulation at greater depths.

Concurrent reduction in pressure losses in the pipe joints as wall thickness increases. P_J decreases from about 0.0032 MPa at 7 mm wall thickness to around 0.0004 MPa at 12 mm. This inverse relationship suggests that increasing the wall thickness improves the hydraulic characteristics of the joints. Pressure drops P_J at the joints increase by a factor of 6.69, which can be explained by the approaching constant internal diameter of the joints as the channel diameter of the pipes decreases (Eq. (7)).

3.6 Dependence of drilling depth H on the outer diameter of drill pipes d_O

When changing the size of drill pipes, the following parameters remain constant: V, λ, ρ, ROP, L_{KH}, L_P (Table 1). For drilling wells with larger diameters, the following drill pipes may be used (Table 6).[64]

Table 7 shows the results of calculations of the dependence of the maximum well depth H on the pipe diameter at fixed flow rate and density of the drilling fluid. Fig. 5 shows the dependence of the flow rate U_P and maximum drilling depth H on the pipe size d_O at a fluid flow rate of Q = 0.05 m^3/s.

As shown in Fig. 5, maximum drilling depth increases non-linearly with increasing pipe diameter, following an exponential growth pattern. Flow velocity decreases monotonically with increasing pipe diameter, starting at approximately 4.3 m/s at the smallest diameter and declining to about 1.7 m/s at the largest diameter. This inverse relationship illustrates a fundamental fluid dynamics principle where velocity decreases as cross-sectional area increases at constant flow rate.

As shown in Table 7, pressure losses at the joints are absent for pipes with diameters greater than 168 mm because drill pipes of such diameters are not manufactured. In these cases, casing pipes with coupling joints and without upset ends are used.[65, 66]

With an increase in pipe diameter, the maximum drilling depth increases by a factor of 18. This is due to a reduction in flow velocity, which in turn decreases pressure losses.

From Table 7, it is evident that pipes with a diameter of 127 mm are unsuitable because the vacuum created by the pump would be entirely consumed by the pressure loss P_{KH}.

A notable feature of drilling at a constant fluid flow rate is the invariance of the upward flow density regardless of the drill pipe size. This is demonstrated by Eq. (14), derived from Eq. (13) by substituting initial values for U_P from Eqs. (4) and (5). In Eq. (14), the terms d_h^2 in the numerator and denominator cancel out:

$$\Delta_F = \frac{D^2(\rho_F - \rho_W)U_D\pi d_p^2}{d_P^2 4Q} \tag{14}$$

Table 6: Dependence of the maximum well depth H on the wall thickness δ of the drill pipe 168 mm.

Outer diameter d_O, mm	127	140	168	178	194	219
Wall thickness, δ mm,	8*	9	9	10	11	11
Inner diameter d_P, mm	111	122	150	158	172	197
Inner diameter of joints d_J, mm	95	101	128	158**	172**	197**

* From several values, one typical size is selected.

** For drilling large-diameter wells, casing pipes without tool joints are used.

Table 7: Dependence of the maximum well depth H on the ROP.

Step number	d_O, m	d_P, m	d_J, m	U_P, m/s (9)	U_J, m/s (9)	H, m (11)	P_{KH}, Pa (2)	P_J, Pa (7)	P_P, Pa (2)
0	0.127	0.111	0.095	0	0	0	70000	0	0
1	0.140	0.122	0.101	4.27	6.23	27	44900	2500	22600
2	0.168	0.150	0.128	2.83	3.88	91	16200	1500	52300
3	0.178	0.158	0.158	2.55	2.55	130	12400	0	57600
4	0.194	0.172	0.172	2.16	2.16	211	8200	0	61800
5	0.219	0.197	0.197	1.64	1.64	476	3900	0	66100

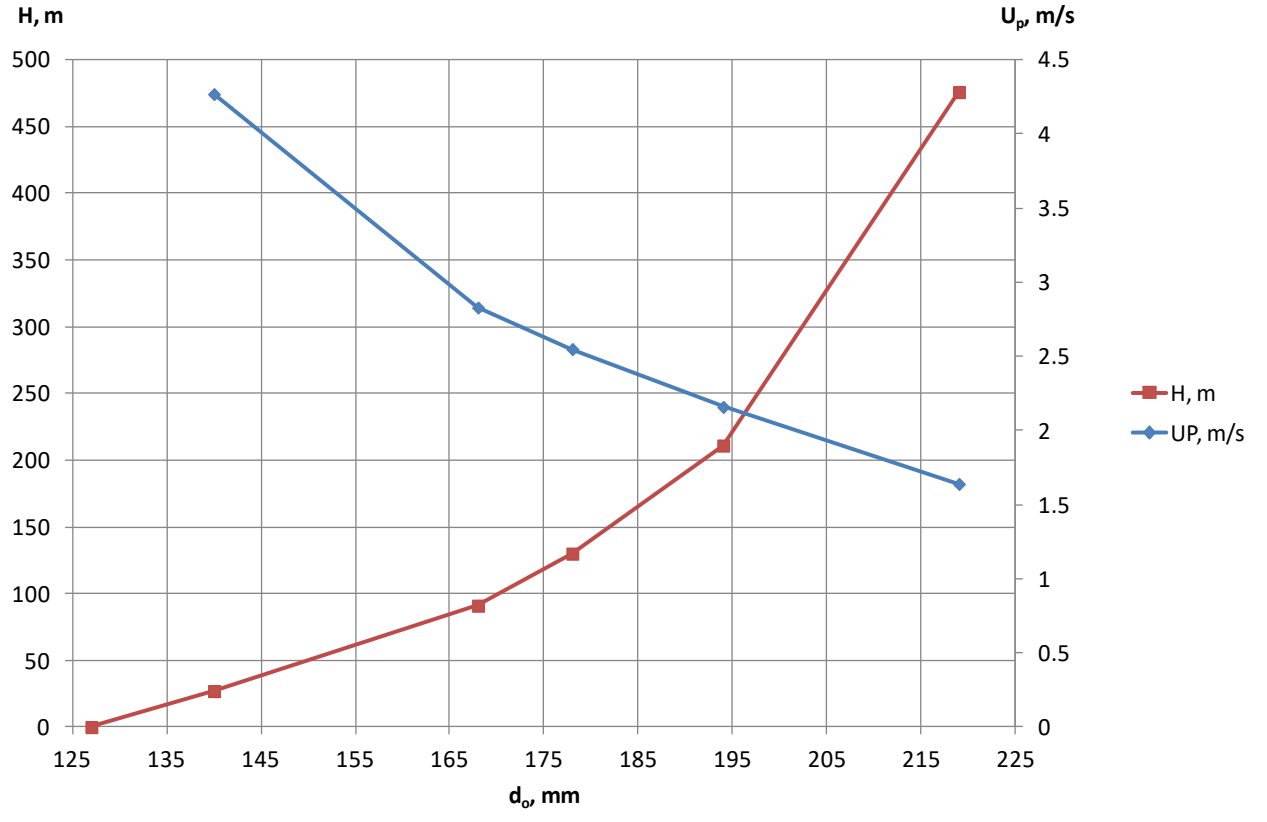

Fig. 5: Dependence of flow velocity U_P and maximum drilling depth H on pipe size d_O at fluid flow rate (q=0.05 m^3).

The aforementioned drawbacks of the constant fluid flow rate Q scenario can be mitigated by using a constant upward flow velocity U_P instead.

Table 8 shows the results of calculations of the dependence of the maximum well depth H on the pipe diameter at a constant upward flow rate. Fig. 6 shows the dependence of the fluid supply Q, flow density ρ and maximum drilling depth H on the pipe diameter d_O at a constant upward flow rate.

As shown in Fig. 6, maximum drilling depth increases linearly with increasing pipe diameter, starting at about 55 meters at 125 mm diameter and reaching approximately 140 meters at 220 mm diameter. Fluid flow rate also increases with pipe diameter, beginning at around 25 L/s at the smallest diameter and rising to about 85 L/s at the largest diameter, following a nearly linear trend. Flow density decreases as pipe diameter increases, starting at approximately 1280 kg/m^3 at 125 mm diameter and declining to about 1090 kg/m^3 at 220 mm diameter.

The advantage of this approach is that it allows the use of 127 mm diameter drill pipes while achieving an acceptable drilling depth of 54 m under the given conditions (Table 8). However, this comes with the trade-off of a high upward flow density of the drilling fluid (1280 kg/m^3).

The present study investigates the dependencies of maximum drilling depth (H) on various operational parameters, including fluid flow rate (Q), pipe wall thickness (δ), and outer diameter of drill pipes (d_o). By systematically analyzing these parameters, we have identified several critical insights that are aligned with previous research while offering novel perspectives.

Table 8: Dependence of maximum drilling depth on pipe diameter at constant upward flow velocity (U_P=2.830 m/s)

Step number	d_O, m	d_P, m	d_J, m	Q, m^3/s (4)	ρ, kg/m^3 (13)	U_J, m/s (9)	H, m (11)	P_{KH}, Pa (2)	P_J, Pa (7)	P_P, Pa (2)
0	0.127	0.111	0.095	0.027	1280	3.94	54	24180	2690	43130
1	0.140	0.122	0.101	0.033	1240	4.13	64	21260	5580	43160
2	0.168	0.150	0.128	0.050	1160	3.88	92	16200	1500	52230
3	0.178	0.158	0.158	0.055	1140	2.83	104	14870	0	55130
4	0.194	0.172	0.172	0.066	1120	2.83	119	13420	0	56580
5	0.219	0.197	0.197	0.086	1090	2.83	139	11350	0	58670

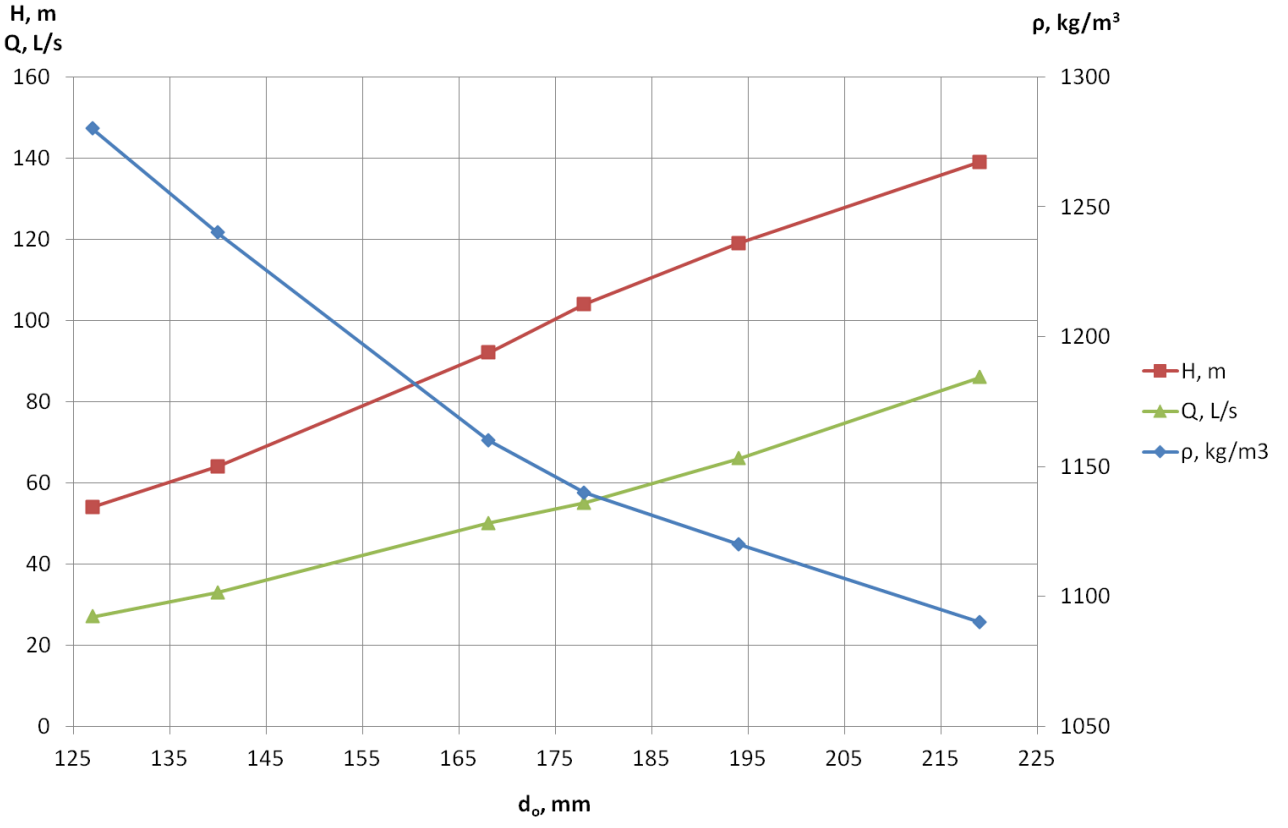

Fig. 6: Dependence of the fluid supply Q, flow density ρ and maximum drilling depth H on the pipe diameter d_O at a constant upward flow rate U_P = 2.93 m/s.

The observed inverse relationship between the maximum drilling depth and fluid flow rate corroborates earlier studies emphasizing the role of flow-induced pressure losses in limiting well depth. Specifically, the rapid decline in drilling depth with increasing flow rate, as demonstrated in Table 2, reflects the compounded effects of pressure losses in smooth and jointed sections of the drill string. This finding underscores the importance of optimizing flow rates to balance effective cuttings transport with manageable pressure losses. Notably, the quadratic dependence of pressure losses on flow velocity suggests that even minor increases in flow velocity can substantially limit drilling depth, an aspect that merits further exploration.

In analyzing the influence of pipe wall thickness, we observed a proportional decrease in maximum depth with increasing δ, as shown in Table 4 and Fig. 4. This phenomenon is attributed to reductions in inner diameter and consequent increases in flow velocity and pressure losses. These results align with theoretical predictions and highlight the need for advanced material technologies to produce pipes with high strength-to-weight ratios and minimal wall thickness.

The relationship between outer diameter (d_o) and drilling depth provides another critical perspective. As illustrated in Table 7, increasing d_o significantly enhances the achievable depth, primarily due to reductions in flow velocity and associated pressure losses. The transition from drill pipes to casing pipes for larger diameters further emphasizes the practical limitations of standard drill string designs and the need for innovations in tool joint engineering.

A key contribution of this study is the proposed methodology for maintaining constant upward flow velocity (Up). This approach mitigates the drawbacks of a constant fluid flow rate, as demonstrated by the acceptable performance of smaller-diameter pipes under these conditions (Table 8). However, the increased upward flow density indicates potential challenges in managing fluid properties and pump capacity, warranting further investigation.

Innovative approaches to enhancing the efficiency of large-diameter well drilling and intensifying formation fluid influx are supported by patented solutions, including an air supply device for backwashing using an air-lift and a device for creating an implosion effect to stimulate fluid influx.[67-70]

The findings also have implications for the broader field of drilling engineering. They highlight the complex interplay between hydraulic parameters and mechanical properties of the drill string, suggesting opportunities for optimization through integrated design approaches. Future research should focus on experimental validation of the proposed models, particularly under varying geological conditions, to enhance their applicability and robustness.

4. Conclusion

This study provides a comprehensive theoretical analysis of the geological and technological factors that influence the

maximum achievable depth in large-diameter well drilling under reverse-circulation conditions. The results demonstrate that increasing the fluid flow rate leads to a reduction in maximum depth due to a quadratic rise in pressure losses, underscoring the need for careful flow optimization to balance effective cuttings transport and hydraulic efficiency. When the fluid flow rate is increased from 1000 to 4000 L/min, *i.e.*, 4 times, the maximum drilling depth decreases from 1190 to 49 meters, *i.e.*, 24 times. The required pressure at the pump outlet gradually decreases from 0.066 MPa to 0.044 MPa, which may seem counterintuitive. However, this is explained by the fact that increasing flow rates reduces the achievable drilling depth, which in turn lowers the total hydraulic resistance along the shortened fluid circulation path.

As ROP increases from 2 to 20 m/h, the maximum drilling depth decreases from approximately 105 m to 76 m. This inverse relationship can be attributed to the greater cuttings generated at higher penetration rates, which require more effective hydraulic transport. To compensate for this, the density of the drilling fluid must be increased from around 1032 kg/m³ to 1310 kg/m³ to maintain adequate carrying capacity and ensure borehole stability. When bottom-hole pressure increases from 0.05 to 0.085 MPa, the permissible drilling depth increases from 57 m to 115 m, and the pressure loss in the annular space grows from 0.033 to 0.067 MPa.

Thicker drill pipe walls negatively affect drilling depth by reducing the inner diameter, which increases flow velocity and pressure losses; therefore, the use of advanced materials that allow thinner walls without compromising strength may improve performance. Increasing the wall thickness of drill pipes from 7 to 12 mm reduces pressure losses in joints from 0.0032 to 0.0004 MPa but also decreases the allowable depth from 101 m to 74 m.

A larger outer pipe diameter significantly enhances drilling depth by lowering flow velocity and minimizing hydraulic resistance—particularly when casing pipes without tool joints are used. Maintaining a constant upward flow velocity enables the use of smaller-diameter pipes while still achieving practical drilling depths, although this approach demands precise control of fluid density and pump operation. Maximum drilling depth increases non-linearly with increasing pipe diameter, following an exponential growth pattern. Flow velocity decreases monotonically with increasing pipe diameter, starting at approximately 4.3 m/s at the smallest diameter and declining to about 1.7 m/s at the largest diameter. This inverse relationship illustrates a fundamental fluid dynamics principle where velocity decreases as cross-sectional area increases at constant flow rate.

A comparative analysis with closely related studies reveals the advantages of the proposed approach. For instance, in conventional large-diameter well drilling techniques, the limiting depth under similar hydraulic conditions rarely exceeds 70–90 meters due to high pressure losses associated with standard drill pipe assemblies.[21] In contrast, the current study demonstrates the possibility of reaching depths up to 476 meters when using casing pipes without tool joints and optimizing outer diameters and flow parameters. Furthermore, while earlier studies focus primarily on empirical relationships,[43,57] our methodology offers a consistent analytical framework grounded in hydraulic principles. The derived formulas enable accurate prediction of pressure losses and achievable depth across a wide range of pipe diameters and wall thicknesses. This analytical rigor allows for a more versatile adaptation to varying geological and technological conditions compared to previous empirical approaches.

These findings are significant because they provide a framework for optimizing reverse-circulation drilling systems in challenging geological environments. The results highlight the need for an integrated approach that balances hydraulic parameters, pipe design, and material selection to improve drilling efficiency. This study can inform future design decisions and technological developments aimed at enhancing the performance and cost-effectiveness of large-diameter water well drilling operations, particularly in arid and hard-to-access regions.

Acknowledgments

This research has been/was/is funded by the Science Committee of the Ministry of Science and Higher Education of the Republic of Kazakhstan (Grant No. AP23487129).

Conflict of Interest

There is no conflict of interest.

Supporting Information

Not applicable.

References

[1] M. T. Biletskiy, B. T. Ratov, V. L. Khomenko, B. R. Borash, A. R. Borash, Increasing the mangystau peninsula underground water reserves utilization coefficient by establishing the most effective method of drilling water supply wells, *Series of Geology and Technical Sciences*, 2022, **5**, 51-62, doi: 10.32014/2518-170x.217.

[2] A. Togasheva, R. Bayamirova, M. Sarbopeyeva, M. Bisengaliev, V. L. Khomenko, Measures to prevent and combat complications in the operation of high-viscosity oils of Western Kazakhstan, *News of the National Academy of Sciences of the Republic of Kazakhstan, Series of Geology and Technical Sciences*, 2024, **1**, 257-270, doi: 10.32014/2024.2518-170X.379.

[3] A. Sudakov, A. Dreus, B. Ratov, Sudakova, O. Khomenko, S. Dziuba, D. Sudakova, S. Muratova, M. Ayazbay, Substantiation of thermomechanical technology parameters of absorbing levels isolation of the boreholes, *NEWS of National Academy of Sciences of the Republic of Kazakhstan*, 2020, **2**, 63-71, doi: 10.32014/2020.2518-170x.32.

[4] A. Sudakov, A. Dreus, B. Ratov, D. Delikesheva, theoretical bases of isolation technology for swallowing horizons using thermoplastic materials, *Series of Geology and Technical*

Sciences, 2018, **2**, 72-80.
[5] G. Umirova, K. Togizov, A. Muzapparova, S. Kisseyeva, Preparation of calculation parameters according to logging data for 19-24 productive horizons of the uzen field, *SGEM International Multidisciplinary Scientific GeoConference, EXPO Proceedings*, July 3-9, Albena, Bulgaria, STEF92 Technology, 2023, **23**, 729-742, doi: 10.5593/sgem2023/1.1/s06.87.
[6] V. L. Khomenko, B. T. Ratov, O. A. Pashchenko, O. M. Davydenko, B. R. Borash, Justification of drilling parameters of a typical well in the conditions of the Samskoye field, *IOP Conference Series*: *Earth and Environmental Science*, 2023, **1254**, 012052, doi: 10.1088/1755-1315/1254/1/012052.
[7] Y. A. Koroviaka, M. R. Mekshun, A. O. Ihnatov, B. T. Ratov, Y. S. Tkachenko, Y. M. Stavychnyi, Determining technological properties of drilling muds, *Naukovyi Visnyk Natsionalnoho Hirnychoho Universytetu*, 2023, **2**, 25-32, doi: 10.33271/nvngu/2023-2/025.
[8] X. H. Xue, Z. M. Su, The optimization program of reverse circulation drilling equipment, *Advanced Materials Research*, 2013, **650**, 634-637, doi: 10.4028/www.scientific.net/amr.650.634.
[9] O. Pashchenko, V. Khomenko, V. Ishkov, Y. Koroviaka, R. Kirin, S. Shypunov, Protection of drilling equipment against vibrations during drilling, *IOP Conference Series*: *Earth and Environmental Science*, 2024, **1348**, 012004, doi: 10.1088/1755-1315/1348/1/012004.
[10] M. T. Biletskiy, B. T. Ratov, V. L. Khomenko, A. R. Borash, S. K. Muratova, The choice of optimal methods for the development of water wells in the conditions of the Tonirekshin field (Kazakhstan), *Naukovyi Visnyk Natsionalnoho Hirnychoho Universytetu*, 2024, **1**, 13-19, doi: 10.33271/nvngu/2024-1/013.
[11] M. L. van der Schans, M. Bloemendal, N. Robat, A. Oosterhof, P. J. Stuyfzand, N. Hartog, Field testing of a novel drilling technique to expand well diameters at depth in unconsolidated formations, *Groundwater*, 2022, **60**, 808-819, doi: 10.1111/gwat.13203.
[12] C. J. Okere, G. Su, J. Zhou, G. Li, C. Tan, Lost circulation control for pump-injected reverse circulation drilling: experimental optimization and theoretical analyses, *IOP Conference Series*: *Earth and Environmental Science*, 2021, **814**, 012005, doi: 10.1088/1755-1315/814/1/012005.
[13] L. H. Zhu, Y. Huang, R. H. Wang, J. Y. Wang, A mathematical model of the motion of cutting particles in reverse circulation air drilling, *Applied Mathematics and Computation*, 2015, **256**, 192-202, doi: 10.1016/j.amc.2014.12.153.
[14] S. Zhou, K. Du, J. Xie, Application of directional circulation drilling and air-lift reverse circulation borehole cleaning, *Yantu Gongcheng Xuebao/Chinese Journal of Geotechnical Engineering*, 2011, **33**, 166-168.
[15] H. Hapich, A. Zahrytsenko, A. Sudakov, A. Pavlychenko, S. Yurchenko, D. Sudakova, I. Chushkina, Prospects of alternative water supply for the population of Ukraine during wartime and post-war reconstruction, *International Journal of Environmental Studies*, 2024, **81**, 289-300, doi: 10.1080/00207233.2023.2296781.
[16] Y. Che, J. Zhou, H. Wu, J. Cheng, Experimental study on the cyclic pressure loss of pump-injected reverse circulation drilling, *Shiyou Huagong Gaodeng Xuexiao Xuebao/Journal of Petrochemical Universities*, 2016, **29**, 27-31, doi: 10.3969/j.issn.1006-396X.2016.02.006
[17] H. Cheng, L. Guo, Z. Yao, Z. Wang, C. Rong, Experimental study on transport law of multiphase slag discharge and optimization of well washing parameters in gas lift reverse circulation of drilling shaft sinking, *Zhongguo Kuangye Daxue Xuebao/Journal of China University of Mining and Technology*, 2024, **53**, 224-237, doi: 10.13247/j.cnki.jcumt.20230101.
[18] B. R. Borash, M. T. Biletskiy, V. L. Khomenko, Y. A. Koroviaka, B. T. Ratov, Optimization of technological parameters of airlift operation when drilling water wells, *Naukovyi Visnyk Natsionalnoho Hirnychoho Universytetu*, 2023, **3**, 25-31, doi: 10.33271/nvngu/2023-3/025.
[19] J. H. van Lopik, T. Sweijen, N. Hartog, R. J. Schotting, Contribution to head loss by partial penetration and well completion: implications for dewatering and artificial recharge wells, *Hydrogeology Journal*, 2021, **29**, 875-893, doi: 10.1007/s10040-020-02228-5.
[20] H. Ju, I.-S. Hwang, Systematic model for estimation of future inadvertent human intrusion into deep rad-waste repository by domestic groundwater well drilling, *Nuclear Engineering and Design*, 2018, **327**, 38-50, doi: 10.1016/j.nucengdes.2017.12.005.
[21] G. J. Houben, Review: hydraulics of water wells: head losses of individual components, *Hydrogeology Journal*, 2015, **23**, 1659-1675, doi: 10.1007/s10040-015-1313-7.
[22] B. Ratov, A. Borash, M. Biletskiy, V. Khomenko, Y. Koroviaka, A. Gusmanova, O. Pashchenko, V. Rastsvietaiev, O. Matyash, Identifying the operating features of a device for creating implosion impact on the water bearing formation, *Eastern-European Journal of Enterprise Technologies*, 2023, **5**, 35-44, doi: 10.15587/1729-4061.2023.287447.
[23] L. Li, D. Ru, K. Li, Y. Wang, Research and application of reverse circulation drilling technology, *International Oil & Gas Conference and Exhibition in China*, December 5-7, Beijing, China, SPE, 2006, SPE-104412-MS, doi: 10.2118/104412-ms.
[24] B. T. Ratov, B. V. Fedorov, V. L. Khomenko, A. R. Baiboz, D. R. Korgasbekov, Some features of drilling technology with PDC bits, *Naukovyi Visnyk Natsionalnoho Hirnychoho Universytetu*, 2020, **3**, 13-18, doi: 10.33271/nvngu/2020-3/013.
[25] M. T. Biletsky, B. T.; Ratov, A. A. Kozhevnykov, A. R. Baiboz, D. N. Delikesheva, Updating the theoretic model of rock destruction in the course of drilling, *News of the National Academy of Sciences of the Republic of Kazakhstan, Series of Geology and Technical Sciences*, 2018, **2**, 63-71.
[26] M. T. Biletsky, A. A. Kozhevnykov, B. T. Ratov, V. L. Khomenko, Dependence of the drilling speed on the frictional forces on the cutters of the rock-cutting tool, *Naukovyi Visnyk Natsionalnoho Hirnychoho Universytetu*, 2019, **1**, 21-27, doi: 10.29202/nvngu/2019-1/22.
[27] Z. Hou, Y. Liu, G. Yang, J. Xia, Air-lift characteristics of rock core mass in gas–liquid–solid mixed flow, *Physics of Fluids*, 2024, **36**, 043322, doi: 10.1063/5.0200638.

[28] X. Yang, B. Guo, T. A. Timiyan, Analytical and numerical simulation of asymmetric converging flow of gas under drill bits in reverse circulation gas drilling, *Journal of Energy Resources Technology*, 2022, **144**, 043201, doi: 10.1115/1.4051551.

[29], B. T. Ratov, V. A. Mechnik, Increasing the durability of an impregnated diamond core bit for drilling hard rocks, *SOCAR Proceedings*, 2024, 24-31, doi: 10.5510/ogp20240100936.

[30] B. T. Ratov, V. L. Khomenko, A. E. Kuttybayev, K. S. Togizov, Z. G. Utepov, Innovative drill bit to improve the efficiency of drilling operations at uranium deposits in Kazakhstan, *Series of Geology and Technical Sciences*, 2024, **4**, 224-236, doi: 10.32014/2024.2518-170x.437.

[31] B. T. Ratov, V. A. Mechnik, V. L. Khomenko, A. O. Ihnatov, A. B. Kalzhanova, Influence of disperse-hardening additive chrome diboride on the structure of carbide matrixes of PDC drill bits, *Naukovyi Visnyk Natsionalnoho Hirnychoho Universytetu*, 2024, **4**, 27-34, doi: 10.33271/nvngu/2024-4/027.

[32] C. S. Wang, L. Zhang, Fluid simulation in a cyclone reverse circulation well washing device based on computational fluid dynamics, *Energy Science & Engineering*, 2019, **7**, 1306-1314, doi: 10.1002/ese3.349.

[33] B. T. Ratov, V. L. Khomenko, M. T. Biletskiy, S. T. Zakenov, Z. S. Makhitova, Modernization of water well drilling technology with drilling fluid reverse circulation, *News of the National Academy of Sciences of the Republic of Kazakhstan, Series of Geology and Technical Sciences*, 2025, **2**, 237-252, doi: 10.32014/2025.2518-170X.453.

[34] Y. Luo, B. Guo, L. Zhang, D. Xiao, Finite element analysis of flow field in drill bit design for gas-lift drilling, *Journal of Energy Resources Technology*, 2021, **143**, 113002, doi: 10.1115/1.4049607.

[35] P. Cao, H. Cao, J. Cao, M. Liu, B. Chen, Studies on pneumatic transport of ice cores in reverse circulation air drilling, *Powder Technology*, 2019, **356**, 50-59, doi: 10.1016/j.powtec.2019.08.001.

[36] R. Wang, L. An, P. Cao, B. Chen, M. Sysoev, D. Fan, P. G. Talalay, Rapid ice drilling with continual air transport of cuttings and cores: General concept, *Polar Science*, 2017, **14**, 21-29, doi: 10.1016/j.polar.2017.09.004.

[37] R. Wang, X. Lv, X. Fan, D. Gong, A. Liu, Key parameters and mechanisms of ice cores autonomously breaking with air reverse-circulation drill systems, *Cold Regions Science and Technology*, 2024, **217**, 104053, doi: 10.1016/j.coldregions.2023.104053.

[38] A. T. Zholbassarova, R. Y. Bayamirova, B. T. Ratov. Development of technology for intensification of oil production using emulsion based on natural gasoline and solutions of nitrite compounds, *SOCAR Proceedings*, 2024, **2**, 48-55, doi: 10.5510/ogp20240200965.

[39] Y. Zhang, J. Zhang, Technical improvements and application of air-lift reverse circulation drilling technology to ultra-deep geothermal well, *Procedia Engineering*, 2014, **73**, 243-251, doi: 10.1016/j.proeng.2014.06.194.

[40] C. Zeng, Y. Chen, X. Yan, Transportation of cuttings through drill rods during reverse-circulation reaming, *Tunnelling and Underground Space Technology*, 2022, **126**, 104544, doi: 10.1016/j.tust.2022.104544.

[41] S. Sun, K. Bo, R. Jia, P. Cao, B. Chen, M. Guo, Experimental investigation and CFD simulation of multiphase flow behavior in air reverse circulation drilling, *Advanced Powder Technology*, 2023, **34**, 104168, doi: 10.1016/j.apt.2023.104168.

[42] K. Polak, K. Górecki, K. Kaznowska-Opala, The dynamics of water wells efficiency reduction and ageing process compensation, *Water*, 2019, **11**, 117, doi: 10.3390/w11010117.

[43] G. J. Houben, J. Wachenhausen, C. R. Guevara Morel, Effects of ageing on the hydraulics of water wells and the influence of non-Darcy flow, *Hydrogeology Journal*, 2018, **26**, 1285-1294, doi: 10.1007/s10040-018-1775-5.

[44] I. Chudyk, D. Sudakova, A. Dreus, A. Pavlychenko, A. Sudakov, Determination of the thermal state of a block gravel filter during its transportation along the borehole, *Mining of Mineral Deposits*, 2023, **17**, 75-82, doi: 10.33271/mining17.04.075.

[45] I. Chudyk, D. Sudakova, A. Pavlychenko, A. Sudakov, Bench studies of the process of transporting an inverse gravel filter of block type along the well, *IOP Conference Series: Earth and Environmental Science*, 2024, **1348**, 012009, doi: 10.1088/1755-1315/1348/1/012009.

[46] H. Song, F. Li, B. Li, J. Guo, J. Li, S. Zhang, Z. Li, Flow law of particles carried by well-flushing fluid in the annulus and prediction of flushing efficiency based on numerical simulation-interpretable machine learning model, *Fuel*, 2025, **392**, 134829, doi: 10.1016/j.fuel.2025.134829.

[47] H. Song, F. Li, B. Li, J. Guo, W. Zhang, Y. Wang, Z. Li, Y. Pan, Research on the wellbore cleaning mechanism and prediction of cleaning ability of well-flushing fluid based on experiment-molecular dynamics simulation-machine learning, *Separation and Purification Technology*, 2025, **359**, 130875, doi: 10.1016/j.seppur.2024.130875.

[48] H. Ye, Z. Lai, L. Tian, R. Zhang, B. Liu, X. Zheng, Air-lifting reverse-circulation drilling in deep geothermal wells and the effect of dual-wall drill pipe depth down the hole, *Energies*, 2025, **18**, 1224, doi: 10.3390/en18051224.

[49] H. Mu, G. Jiang, J. Sun, Y. He, T. Dong, W. Zhang, Q. Wang, Prediction of ROP-increasement and lost circulation prevention effect by drilling fluid based on GS-XGBoost, *Computational and Experimental Simulations in Engineering*, Cham: Springer Nature Switzerland, 2025, 81-92, doi: 10.1007/978-3-031-81673-4_6.

[50] M. T. Biletskiy, B. T. Ratov, V. L. Khomenko, A. Y. Yesturliyev, Z. S. Makhitova, Improved techniques for exploration of groundwater deposits for conditions of rural areas of the Mangystau Peninsula, *Naukovyi Visnyk Natsionalnoho Hirnychoho Universytetu*, 2025, **1**, 5-12, doi: 10.33271/nvngu/2025-1/005.

[51] Y. Xu, D. Zhang, T. Xian, Z. Ma, H. Gao, Y. Ma, Two-

direction prediction method of drilling fluid based on OS-ELM for water well drilling, *Journal of Advanced Computational Intelligence and Intelligent Informatics*, 2023, **27**, 594-602, doi: 10.20965/jaciii.2023.p0594.
[52] A. Chakraborty, Water well drilling, well construction and well development, *Groundwater Development and Management*, Cham: Springer International Publishing, 2018, 243-266, doi: 10.1007/978-3-319-75115-3_10.
[53] S. Hapugoda, J. Manuel, Techniques used and problems encountered in normal and reverse circulation drilling at the Mt Roseby Project, Cloncurry, North West Queensland, *XXV International Mineral Processing Congress 2010*, 2010, **4**, 2865-2879.
[54] L. Guo, H. Cheng, Z. Yao, C. Rong, G. Yang, X. Wang, Y. Fang, B. Xie, Study on the flow field of multi-phase coupling slag discharge and the influencing factors of slag discharge effect in gas lift reverse circulation of drilling shaft sinking, *International Journal of Coal Science & Technology*, 2024, **11**, 82, doi: 10.1007/s40789-024-00732-7.
[55] N. Sun, T. Ye, R. Wang, Direct simulations of bedrock core and cuttings transport phenomena in reverse circulation drilling, *Physics of Fluids*, 2024, **36**, 123102, doi: 10.1063/5.0237827.
[56] Q. Li, X. Zhang, Z. Li, J. Li, F. Dai, Annular aerated gas-lift reverse circulation drilling technology and key parameters design, *Xinan Shiyou Daxue Xuebao/Journal of Southwest Petroleum University*, 2021, **43**, 35-43. doi: 10.11885/j.issn.16745086.2021.04.29.01
[57] J. Macuda, J. Siemek, S. Wysocki, M. Gaczoł, The impact of modern drilling fluids on improving the hydraulic efficiency of water wells, *Gospodarka Surowcami Mineralnymi/Mineral Resources Management*, 2018, **34**, 133–144. doi: 10.24425/122587.
[58] G. P. Beretta, M. Baio, Proposal of Guidelines for field description and classification of porous sediments from water well drilling - *in situ* fast procedure - ver 1.0, *Acque Sotterranee - Italian Journal of Groundwater*, 2020, **9**, 39-50, doi: 10.7343/as-2020-463
[59] A. Kozhevnykov, V. Khomenko, B. C. Liu, O. Kamyshatskyi, O. Pashchenko, The history of gas hydrates studies: from laboratory curiosity to a new fuel alternative, *Key Engineering Materials*, 2020, **844**, 49-64, doi: 10.4028/www.scientific.net/kem.844.49.
[60] B. Ratov, A. Kosminov, A. Kuttybayev, M. Tabylganov, M. Seksenbay, Public-private partnership between satbayev university and SK geoservice LLP: enhancing collaboration in technological innovation and production, *E3S Web of Conferences*, 2024, **525**, 01007, doi: 10.1051/e3sconf/202452501007.
[61] L. Guo, H. Cheng, Z. Yao, C. Rong, Z. Wang, X. Wang, CFD–DEM method is used to study the multi-phase coupling slag discharge flow field of gas-lift reverse circulation in drilling shaft sinking, *Scientific Reports*, 2024, **14**, 13853, doi: 10.1038/s41598-024-64519-1.
[62] V. Khomenko, O. Pashchenko, B. Ratov, R. Kirin, S. Svitlychnyi, A. Moskalenko, Optimization of the technology of hoisting operations when drilling oil and gas wells, *IOP Conference Series: Earth and Environmental Science*, 2024, **1348**, 012008, doi: 10.1088/1755-1315/1348/1/012008.
[63] A. V. Pavlychenko, A. O. Ihnatov, Y. A. Koroviaka, B. T. Ratov, S. T. Zakenov, Problematics of the issues concerning development of energy-saving and environmentally efficient technologies of well construction, *IOP Conference Series: Earth and Environmental Science*, 2022, **1049**, 012031, doi: 10.1088/1755-1315/1049/1/012031.
[64] N. Tileuberdi, I. Gussenov, Review on miscible, immiscible, and progressive nitrogen injection for enhanced oil recovery, *Energy Reports*, 2024, **12**, 360-367. doi: 10.1016/j.egyr.2024.06.004
[65] N. Tileuberdi, B. Nassibullin, Zh. Kuli, I. Gussenov, Sh. Kenzhekhanov, X. Yin, and Y. Sailaukhanuly, Challenges of gel treatment application for conformance control, *Engineered Science*, 2024, **31**, 1238, doi: 10.30919/es1238.
[66] X. Ma, Y. Chen, L. Qi, Research and application of gas-lift reverse circulation drilling technology to geothermal well construction in Dalian Jiaoliu Island, *Procedia Engineering*, 2014, **73**, 252-257, doi: 10.1016/j.proeng.2014.06.195.
[67] B. T. Ratov, M. T. Biletskiy, B. R. Borash, A.R. Borash, Air supply device for well drilling with backwashing using air lift, *Republic of Kazakhstan*, 2022.
[68] M. T. Biletskiy, B. T. Ratov, A.R. Borash, B.R. Borash, Device for intensifying the influx of formation fluid into the well, *Republic of Kazakhstan*, 2022.
[69] N. Tileuberdi, B. Nassibullin, A. Yskak, I. Gussenov, Permeability damage induced by low and high molecular weight polymer gels in porous media, *Engineered Science*, 2024, **29**, 1092, doi: 10.30919/es1092.
[70] N. Tileuberdi, A. N. AL-Dujaili, M. Mashrapova, K. Togizov, M. Sanatbekov, A. Yergali, Optimizing oil recovery by low-pressure nitrogen injection: an experiment case study, *ES Materials & Manufacturing*, 2024, **25**, 1189, doi: 10.30919/esmm1189.